Time-Stable Receiving System With Local Digitization Based on a Dithered Sample Clock

Kai Wang, Wei Wei ⓘ, Danyang Wang, Pengyu Wang, Weilin Xie ⓘ, *Member, IEEE*, and Yi Dong ⓘ

Abstract—We present a time-stable receiving system for broadband signals transmitted via a 25 km fiber optic link. The timing jitter of the signal induced by the transmission link is precisely eliminated after the signal is digitized with a dithered sample clock. The dithered clock is generated from the phase of a voltage-controlled oscillator, introducing the same transmission timing jitter of the link. Therefore, it can withstand an unlimited range of transmission delay variations without using any optical or electrical delay lines. Experimentally, binary phase-shift keying signals with bandwidths of several hundred MHz and different carrier frequencies are transmitted and received by the proposed system. The root mean square of the calculated timing jitters of the received signals is decreased to the order of picosecond. The simple remote end and immunity to environmental perturbations of the proposed scheme make it an ideal candidate for a large-scale distributed antenna system.

Index Terms—Time-stabilized signal transfer, broadband receiving system, synchronized digitization.

I. INTRODUCTION

COMPARED with a traditional single antenna detection scheme, the distributed antenna system offers superior signal-to-noise ratio enhancement, a larger effective aperture, and the capability of precise positioning, thereby recently attracting great attention [1], [2]. For a distributed antenna system as shown in Fig. 1, multiple remote ends together receive signals transmitted from the same target and aggregate them to the local end for further processing. The distance between the remote antenna end and the local end can be tens of kilometers in the practical application, to greatly improve the effective aperture of the system [3]. Fiber optic links are considered the ideal signal transmission medium for such long distance, due to their low loss, immunity to electromagnetic interference, and many other advantages [4]. However, various environmental perturbations will lead to the delay drift of the transmission in the optical fiber link, which will cause the phase jitter in the signal transmitted
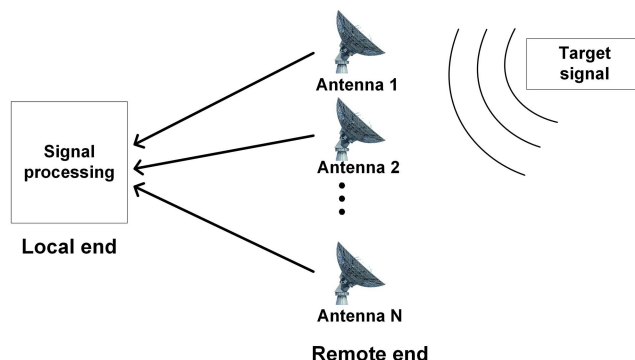

Fig. 1.   The diagram of the distributed antenna system.

to the local end, hindering the subsequent signal combining and precise target location [5]. The longer distance and drastic environmental variations will increase this timing jitter dramatically [6].

To eliminate the influence of the delay variation, the direct solution is to digitize the antenna signal at the remote end and send the digital signal to the local end [7]. However, strict multi-end time synchronization signals are required for the remote digitizers [8]. Meanwhile, the analog-to-digital conversion error will be increased due to the reference voltage drift of the ADC under the influence of ambient temperature changes [9]. Therefore, digitization at remote ends increases the structural complexity but with poor performance. Time-stable receiving at the local station that is immune to transfer delay variation is highly desired.

Several methods have been proposed to stably transmit the microwave signal over the optic fiber link, which can be roughly categorized into two types. One is to compensate for the phase variation of the signal through passive phase mixing or with active phase-locking compensation [10], [11]. For an active phase-locking scheme, a voltage-controlled oscillator (VCO) is often used to generate a frequency signal with an adjustable phase that compensates for the phase variation induced by the fiber transmission. Previously, we have successfully transmitted a 10 GHz signal based on VCO tuning with high stability [12], [13]. By mixing an intermediate frequency (IF) VCO with a high-frequency radio frequency (RF) signal, the control precision and the transfer stability have been evidently improved. Although these phase-adjusting methods have an infinite range of compensation, it can provide a stable transmission only for a single-frequency signal. Note that the receiving antenna signals

Kai Wang, Wei Wei, Danyang Wang, Weilin Xie, and Yi Dong are with the Beijing Institute of Technology, Beijing 100081, China, and also with the Yangtze Delta Region Academy of Beijing Institute of Technology, Jiaxing 314011, China (e-mail: wangk@bit.edu.cn; weiwei@bit.edu.cn; 3220190427@bit.edu.cn; wlxie@bit.edu.cn; yidong@bit.edu.cn).

Pengyu Wang is with the Beijing Institute of Technology, Beijing 100081, China (e-mail: 3120200575@bit.edu.cn).

are always broadband signals, and each frequency component experiences different phase variations due to the link delay variation, which cannot be directly compensated for at the same time based on a phase-adjusting method. The other way is to compensate for the delay variation of the fiber link with an optical/electrical delay line [14], [15] or a wavelength-tunable laser [16]. It can stably transmit a broadband signal because it insures a fixed transmission delay of the link, but its compensation range and speed are limited.

In this paper, we demonstrate a locally digitized, time-stable receiving system for antenna signals transmitted over a 25 km fiber link with an adjustable received frequency range [17]. The signal is transmitted and sampled with a well-controlled dithered clock which experiences the same transmission timing drift as the transmitted signal. Therefore, the transmission timing jitter of the signal is naturally eliminated after the signal is sampled by the analog to digital converter (ADC). Experimentally, binary phase-shift keying (BPSK) signals in different bands are first stably transmitted and then digitized at the local end. The root mean square (RMS) timing jitters of the received signals are reduced by a factor of about 1000 to merely picosecond scale. The proposed receiving system can withstand unlimited transmission delay variation of the link while with a simple remote structure, which is highly suitable for large-scale distributed detection systems in severe environments.

II. PRINCIPLE

The purpose of the proposed system is to obtain stable digital signals after local digitization with immunity to the large transmission delay variation of the link so that subsequent signal combining and processing can be performed in the distributed antenna system. Considering the limited compensation range of the optical and electrical delay line and the unlimited adjusting range of the single-frequency signal, we manage to control the phase of a single frequency sample clock instead of directly controlling the transmission delay.

Usually, when the ADC samples a signal, the sampling instant is determined by the rising or falling edge of a phase-stable sample clock. Thus the signal is sampled with a fixed sampling interval. However, if the sample clock has a timing jitter of $\Delta\tau$, the sampling moment would also change by the same time of $\Delta\tau$. In this case, the signal digitized in the ADC will equivalently have a timing jitter of $-\Delta\tau$ accordingly. If the signal to be sampled has already experienced a transmission delay jitter of $\Delta\tau$ in advance, this timing jitter will be naturally eliminated after being sampled in the ADC with the dithered sample clock.

To eliminate the timing jitter of the signals induced by the fiber link, the transmission delay drift of the link should be detected and then used to adjust the sample clock accordingly. Here, it should be emphasized that although different frequency components in a broadband signal have different transmission delays mainly due to the chromatic dispersion, their transmission delay variation can be regarded as the same in quite a large frequency range [18]. As shown in Fig. 2, two steps are carried out to generate this dithered clock. First, a local oscillator (LO) signal is stably transmitted from the local end to the remote
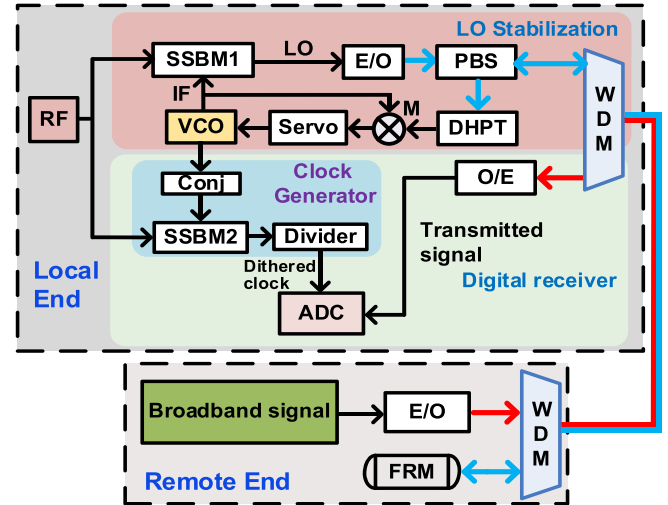

Fig. 2. Schematic diagram of the time-stable receiving system. E/O: Electrical to optical conversion; O/E: Optical to electrical conversion; FRM: Faraday rotator mirror; WDM: Wavelength division multiplexer, SSBM: Single-sideband modulator; M: Mixer; PD: Photodetector; IF: Intermediate Frequency; DHPT: Dual-heterodyne phase-error transfer, PBS: Polarization beam splitter, Conj: Phase conjugate circuit.

end by using use a VCO-based compensation system, which is shown in the LO stabilization module. Second, this stable LO is transmitted together with the broadband signal back to the local end, experiencing the same transmission delay variation. When returned to the local end, the phase drift of the LO is extracted to generate the dithered clock, digitizing the received broadband signal for delay jitter elimination as shown in the digital receiver module.

For the LO stabilization module, the LO signal is generated by up-converting an RF signal with an IF VCO signal in a single sideband modulator (SSBM). When transmitted to the remote end, it can be expressed as

$$E_{LO} = \cos\left[\omega_{LO} * (t + \Delta\tau_p) + \varphi_{vco}(t)\right]. \qquad (1)$$

ω_{LO} is the angular frequency of the LO signal, which is equal to $\omega_{RF} + \omega_{VCO}$; $\varphi_{vco}(t)$ is the phase of the VCO; $\Delta\tau_p$ is the variable transmission delay of the fiber link.

After the LO signal is transmitted back, the phase drift induced from the link is transferred to an IF signal by the dual-heterodyne phase-error transfer (DHPT) structure [19]. Finally, this phase variation information is used to drive a servo, adjusting the phase of the VCO output for phase compensation. Here, the Faraday rotator mirror at the remote end is used to fix the polarization state of the returned LO light, reducing the power variation of the beat signal and the delay drift related to polarization mode dispersion. When the loop is phase-locked,

$$\omega_{LO} * 2\Delta\tau_p + 2 * \varphi_{vco}(t) = \varphi_{Rb}. \qquad (2)$$

Since φ_{Rb} is the initial constant phase of the rubidium clock, the LO has a stable phase at the remote end, and the phase fluctuation of the LO induced by the link is equal to the conjugation of the VCO phase. Thus the VCO signal can be used to generate the dithered clock which carries the delay variation of the link.
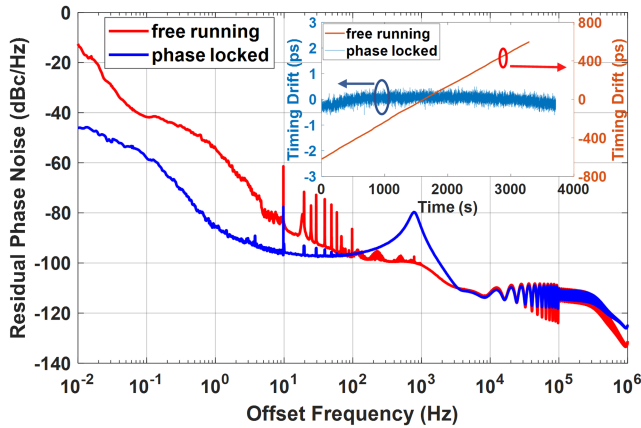
Although the RF to IF conversion both in LO generation and the phase detection will increase the complexity of the proposed scheme compared with previous work, the stability of the LO transmission has been greatly improved.

For the dithered clock generation, the phase-conjugated signal of the VCO is first generated by mixing the VCO output with a frequency-doubled stable reference, which can be expressed as

$$E_{Conj} = \cos\left[\omega_{vco} * t - \varphi_{vco}(t)\right]. \tag{3}$$

Now it represents the phase drift of the LO signal induced by the delay variation of the link. To convert it to the timing drift of the link, the E_{Conj} is up-converted with the RF signal to the frequency of the LO, which can be expressed as

$$E_{LO-J} = \cos[\omega_{LO} * t - \varphi_{vco}(t)] = \cos[\omega_{LO} * (t + \Delta\tau_p)]. \tag{4}$$

Finally, it is divided into the frequency of the sample clock as

$$E_{DClk} = \cos\left[\omega_{LO}/_n * (t + \Delta\tau_p)\right], \tag{5}$$

where n is the ratio of the LO frequency to the sample clock frequency of the ADC, and the dithered clock carrying the delay variation of the link is obtained.

For the antenna signal receiving, the signal is first modulated on the light at the remote end and is then transmitted back to the local end together with the LO signal. Since at any sampling instant of the ADC, the dithered clock and the transmitted signal experience the same delay jitter $\Delta\tau_p$, this common delay jitter can be naturally eliminated no matter how large it will be. Here, we regenerate this dithered clock instead of using the returned LO because the regenerated clock has better noise performance and a higher power level.

It should be noted that the signal with a higher carrier frequency can be directly down-converted to the receiver bandwidth by using the stable LO signal with adjustable frequency at the remote end. Thus, the receiving frequency range is greatly expanded.

The proposed scheme transforms the time-stable broadband transmission requirement into a phase-stable single-frequency stabilization system with high control precision and unlimited compensation range, making it an ideal candidate for applications in severe environments. Here, the VCO-based frequency transfer is not only used to transmit a stable LO signal to the remote end as in a traditional single-frequency transfer system but is also used to extract the phase jitter introduced by the link to generate the sample clock carrying the delay variation of the link. The localization of the signal digitization further simplifies the system structure and alleviates its additional instability and inconsistency.

III. EXPERIMENT AND RESULT

The diagram of the experimental setup is shown in Fig. 3, consisting of a local end and a remote end which are connected via a 25 km fiber link. The local end can be further divided into a stable LO stabilization module and a digital receiver. For the LO stabilization, Laser1 with a wavelength of 1550 nm is split into two parts. One part is amplitude modulated as a local reference light in MZM2 by an adjustable RF signal with the initial

Fig. 3. Experimental setup. MZM: Mach–Zehnder modulator; SSBM: Single-sideband modulator; PBS: Polarization beam splitter; OPMC: Optical polarization-maintaining coupler; AOFS: Acousto-optic frequency-shifter; LF: Loop filter; VCO: Voltage-controlled oscillator; PD: Photodetector; PFD: Digital phase and frequency discriminator; SMF: Single-mode fiber; EF: Electric filter; M: Mixer; Conj: Phase conjugate circuit; PNA: Phase noise analyzer; TIA: Time interval analyzer; AWG: Arbitrary waveform generator; PRFM: Partial reflective Faraday mirror.

frequency set to 9.99 GHz from a microwave source (shown as RF1 in Fig. 3) synchronized with a 10 MHz rubidium clock. The other part is amplitude modulated as the LO signal in MZM1. Its 10 GHz driving signal is generated by up-converting the RF1 signal with a 10 MHz IF VCO signal in SSBM1. The LO light is sent to the S-polarized light port of the polarization beam splitter (PBS) and then injected into a wavelength division multiplexer (WDM) and the fiber link consecutively from the combining port of the PBS. Then it is transmitted to the remote end, and part of the signal is detected with a high-speed photodetector (PD3) for performance evaluation. The stable LO signal at the remote end can also be used for down-converting the antenna signal. The other part is reflected by the partial reflective Faraday mirror (PRFM), rotating the polarization of the returned LO light by 90 degrees. Then the returned LO light goes through the OPMC from the P-polarized light port of the PBS and then beats the reference light in a DHPT structure, generating the IF signal which carries exactly the phase jitter of the returned LO signal but with a lower frequency. This IF signal is used for feedback controlling the phase of the VCO via a well-designed PLL, ensuring the stability of the LO at the remote end. Note that the acousto-optic frequency-shifter is used to prevent the effect of the Rayleigh backscattering.

The digital receiver part is used to digitize the received antenna signal with the dithered sample clock that carries the information of the transmission timing jitter. The dithered clock is generated by upconverting the RF1 signal with the phase-conjugated VCO signal in SSBM2. Here we use an ADC with a 1 GHz sample clock and 2 GHz sample frequency (Teledyne SP Devices ADQ14), thus the up-converted signal is initially divided by 10 with a well-designed electrical divider, realizing the 1 GHz dithered clock. The detection signal within the ADC bandwidth is first generated by an arbitrary waveform generator

Fig. 4.   Residual phase noise and timing drift of the remote 10 GHz LO signal in conditions of phase-locking and free running.
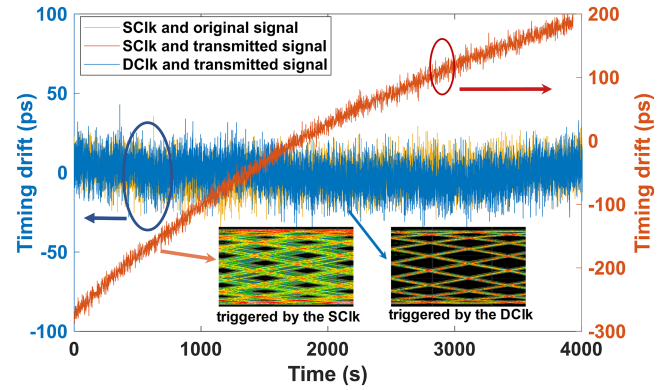

Fig. 5.   Relative timing drift between the single frequency signal and the sample clock in different conditions. SClk: The stable clock; DClk: The dithered clock.

(AWG) at the remote end and is then modulated on the light from Laser2 with the wavelength of 1552 nm. It is transmitted to the local end through the fiber link and the WDM successively and is then detected by PD2. After being sampled by the ADC using the dithered clock, the digitized signal is further processed for performance evaluation. Then, when the detection signal exceeds the ADC bandwidth, it can be down-converted by the stably transmitted adjustable LO signal into the ADC bandwidth, which will be presented in the last paragraph of this section.

The stability of the remote LO signal directly determines the consistency between the transmitted signal and the dithered clock, therefore is first evaluated. Since the frequency limitation of the phase noise analyzer (Symmetricom 5125A), the 10 GHz LO signal at the remote end is down-converted to 10 MHz by mixing it with the 9.99 GHz reference as shown in Fig. 3. The residual phase noises of the remote LO in conditions of free running and phase-locking are shown in Fig. 4. At the lower frequency offset, the phase noise of the free-running system is mainly caused by the ambient temperature changes, contributing to slow and continuous phase drift. Large phase noise spikes from 10 Hz to 100 Hz are also clearly observed, which are mainly caused by environmental vibrations and electrical noises. After phase locking, the phase noise within the loop bandwidth of ∼1 kHz has been effectively suppressed. The residual phase noise reaches -46 dBc/Hz and -87 dBc/Hz at 0.01 Hz and 1 Hz frequency offset, respectively. Compared with the free-running system, they are reduced by over 33 dB, indicating superior long-term stability. The integrated RMS timing jitter of the LO signal from 0.01 Hz to 1 MHz frequency offset is merely 59 fs. The inset shows the timing drift of the down-converted LO signal at the remote end, which is measured by a time interval analyzer (TIA, GuideTech GT668). The TIA can measure the time interval between two single-frequency signals by capturing their rise edges with 1 ps resolution and 3.5 ps noise floor. Note that the timing drift has been magnified by a thousand times for the 10 MHz signal which is down-converted from the 10 GHz LO, the measurement precision can reach the level of femtosecond. While the timing drift is as large as 1211 ps in the condition of free running, the peak to peak timing drift of the phase-locked LO signal is just 1.1 ps within 3700 s.

Then the synchronization between the received signal and the generated dithered clock at the local end is first evaluated with a single frequency signal. Considering the sampling rate of the ADC and the frequency limitation of the TIA, a 250 MHz single frequency signal is generated by the AWG as the original signal at the remote end, which is then transmitted to the local end referred to as the transmitted signal. A phase-stable 1 GHz signal is generated by another microwave source as the stable sample clock, which is used for performance comparison with the generated dithered clock at the local end. The relative timing drift between the original untransmitted signal and the stable clock as in a normal digitization process, the transmitted signal and the stable clock, the transmitted signal and the dithered clock are measured directly using the TIA as shown in Fig. 5. The RMS relative timing jitter between the original untransmitted signal and the stable clock is 8.0 ps, which almost reaches the precision limitation of the TIA. After 25 km transmission, if still using a stable clock for sampling, the drift is increased to 480 ps even in a relatively stable lab environment. When using the dithered clock, however, the drift is dramatically decreased to 9.1 ps, which has no evident deterioration compared with the original untransmitted signal sampled by a stable clock. It proves that the dithered clock keeps good consistency with the transmission timing jitter introduced into the transmitted signal, which means that the delay variation induced by the transmission link has been eliminated. The two insets show the superimposed waveforms of the transmitted 250 MHz captured by a real-time oscilloscope within 10 min triggered by the stable clock and the dithered clock, respectively. Evident slipping can be observed between the stable clock and the transmitted signal while the eye diagram triggered by the dithered clock is thin and clear, proving again that a time-stable transmitted signal can be obtained by using the dithered clock.

Since the ADC has an analog bandwidth of 1 GHz, to verify the stability of the proposed system receiving broadband signals, a 500 Mbps BPSK signal with a 700 MHz carrier is generated by the AWG and tested as shown in Fig. 6. Two ADCs are used to sample the broadband signals before and after the transmission every 10 s, respectively. The sampling duration is 10 ms. The delay drift between the two broadband signals can be calculated
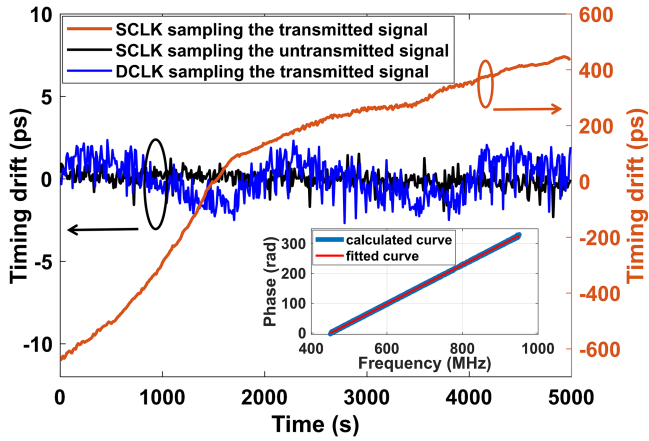
Fig. 6. Timing drift of broadband signals sampled by ADCs in different conditions. SClk: The stable clock; DClk: The dithered clock.
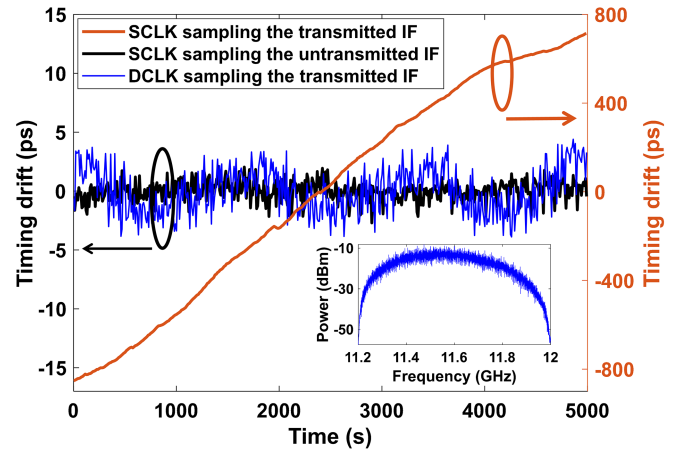

Fig. 7. Timing drift of X-band signals received by the stable receiving system in different conditions. SClk: The stable clock; DClk: The dithered clock.

with the cross-correlation operation in the frequency domain using the sampled data. As shown in the inset, the slope of the fitted curve can be regarded as the precise transmission delay value. Since the signal bandwidth is merely 500 MHz, the chromatic dispersion related delay variation can be reasonably ignored. First, we split the original signals into two parts and sample them with 2 ADCs simultaneously as the untransmitted signals. In this condition, the calculated RMS timing jitter is 0.5 ps, which can be regarded as the noise floor of the digital receiver. The signal-to-noise ratio of the signal, the synchronization performance between the two ADCs both influence the calculated result. After transmission, the timing drift is increased to 1070 ps during 5000 s using a stable clock for sampling. The continuous increase of the timing drift is due to the temperature rise in the lab. When using the dithered clock, as a contrast, the RMS timing drift is merely 1.1 ps. This result is very close to the precision limit of the noise floor, proving that the proposed receiving system can effectively eliminate the timing drift of the broadband signal induced by the link.

To verify the scalability of the receiving frequency range, an X-band 400 Mbps BPSK signal with an 11.6 GHz carrier frequency is generated to simulate a practical imaging radar signal. The RF1 signal is adjusted to 10.99 GHz, and the 11 GHz LO signal is used to down-convert the remote X-band signal within the ADC bandwidth, which is then transmitted to the local end for stable receiving. Accordingly, the division ratio of the frequency divider in the digital receiver module is set to 11. The stability of the received IF signal is shown in Fig. 7, and the spectrum of the signal is in the inset. The RMS timing jitter of the untransmitted IF signal sampled by the stable clock is 0.9 ps. After transmission, the timing drift is increased to 1640 ps during 5000 s when still using the stable clock. While with the dithered clock, the RMS timing drift has been greatly reduced to merely 1.9 ps, which has no obvious degradation compared with the direct digitization of a signal within the ADC bandwidth. It proves again the high stability of the transmitted LO signal at the remote end. Note that the carrier frequency of the received signal is only limited by the frequency range of the LO signal, and the bandwidth of the received signal is only limited by the ADC bandwidth.

V. CONCLUSION

In summary, we propose a time-stable broadband receiving system with a simple remote end which is immune to the transmission delay variation. By generating a dithered clock carrying the same transmission timing jitter of the link as the sample clock for local digitization, the timing jitter is inherently eliminated no matter how large the variation is. Experimentally, Two BPSK signals in different bands with bandwidths of hundreds of megahertz as the practical antenna signals are transmitted via a 25 km fiber link. The RMS timing jitter of the sampled signal is reduced to 1.1 ps and 1.9 ps, respectively. The proposed system perfectly suits the requirement of distributed antenna systems with considerable remote ends in severe environments.

REFERENCES

[1] K. M. Cuomo, S. D. Coutts, J. C. McHarg, N. B. Pulsone, and F. C. Robey, "Wideband aperture coherence processing for next generation radar (NexGen)," MIT Lincoln Lab., Lexington, MA, USA, Tech. Rep. ESC-TR-2004–087, 2004.

[2] F. Zhang, B. Gao, and S. Pan, "Photonics-based MIMO radar with high-resolution and fast detection capability," *Opt. Exp.*, vol. 26, no. 13, pp. 17529–17540, 2018, doi: 10.1364/OE.26.017529.

[3] Y. He et al., "Long-distance telecom-fiber transfer of a radio-frequency reference for radio astronomy," *Optica*, vol. 5, no. 2, pp. 138–146, 2018, doi: 10.1364/OPTICA.5.000138.

[4] R. Esman, S. Pappert, B. Krantz, and G. Gopalakrishnan, "Photonics for microwave generation, transmission, and processing," in *Proc. OSA Opt. Fiber Commun. Conf.*, 2009, pp. 1–3, doi: 10.1364/OFC.2009.OTuA5.

[5] H. Wang, S. Li, X. Xue, X. Xiao, and X. Zheng, "Distributed coherent microwave photonic radar with a high-precision fiber-optic time and frequency network," *Opt. Exp.*, vol. 28, no. 21, pp. 31241–31252, 2020, doi: 10.1364/OE.405465.

[6] Ł. Śliwczyński, P. Krehlik, and M. Lipiński, "Optical fibers in time and frequency transfer," *Meas. Sci. Technol.*, vol. 21, no. 7, 2010, Art. no. 075302, doi: 10.1088/0957-0233/21/7/075302.

[7] M. Zhang, Y. Ji, Y. Zhang, Y. Wu, H. Xu, and W. Xu, "Remote radar based on chaos generation and radio over fiber," *IEEE Photon. J.*, vol. 6, no. 5, Oct. 2014, Art no. 7902412, doi: 10.1109/JPHOT.2014.2352628.

[8] V. Jamnejad, J. Huang, B. Levitt, T. Pham, and R. Cesarone, "Array antennas for JPL/NASA deep space network," in *Proc. IEEE Aerosp. Conf.*, MT, USA: Big Sky, vol. 2, 2002, pp. 2-911-2–921, doi: 10.1109/AERO.2002.1035672.

[9] N. Saputra, M. A. P. Pertijs, K. A. A. Makinwa, and J. H. Huijsing, "12-bit accurate voltage-sensing ADC with curvature-corrected dynamic reference," *Electron. Lett.*, vol. 46, no. 6, pp. 397–398, 2010, doi: 10.1049/el.2010.3337.

[10] Z. Li, L. Yan, B. Luo, and W. Pan, "Phase fluctuation cancellation for uplink radar arrays based on passive frequency mixing," *IEEE Photon. J.*, vol. 10, no. 2, pp. 1–7, Apr. 2018, doi: 10.1109/JPHOT.2018.2815769.

[11] M. Fujieda, M. Kumagai, T. Gotoh, and M. Hosokawa, "Ultrastable frequency dissemination via optical fiber at NICT," *IEEE Trans. Instrum. Meas.*, vol. 58, no. 4, pp. 1223–1228, Apr. 2009, doi: 10.1109/tim.2008.2008088.

[12] X. Wang, Z. Liu, S. Wang, D. Sun, Y. Dong, and W. Hu, "Photonic radio-frequency dissemination via optical fiber with high-phase stability," *Opt. Lett.*, vol. 40, no. 11, pp. 2618–2621, Jun. 2015, doi: 10.1364/OL.40.002618.

[13] S. Wang et al., "Distribution of high-stability 10 GHz local oscillator over 100 km optical fiber with accurate phase-correction system," *Opt. Lett.*, vol. 39, no. 4, pp. 888–891, Feb. 2014, doi: 10.1364/OL.39.000888.

[14] P. Krehlik, L. Sliwczynski, L. Buczek, and J. Kolodziej, "Fiber-optic UTC(k) timescale distribution with automated link delay cancelation," *IEEE Trans. Ultrason., Ferroelect., Freq. Control*, vol. 66, no. 1, pp. 163–169, Jan. 2019, doi: 10.1109/TUFFC.2018.2878319.

[15] O. Lopez, A. Amy-Klein, M. Lours, C. Chardonnet, and G. Santarelli, "High-resolution microwave frequency dissemination on an 86-km urban optical link," *Appl. Phys. B*, vol. 98, no. 4, pp. 723–727, 2010, doi: 10.1007/s00340-009-3832-1.

[16] A. Zhang et al., "Phase stabilized downlink transmission for wideband radio frequency signal via optical fiber link," *Opt. Exp.*, vol. 22, no. 18, pp. 21560–21566, 2014, doi: 10.1364/OE.22.021560.

[17] K. Wang, W. Wei, P. Whang, C. Ma, W. Xie, and Y. Dong, "Phase-stable broadband remote receiving system based on a dithered sample clock," presented at the 2022 Int. Topical Meeting on Microw. Photon. (MWP), Florida, USA, Oct. 2022.

[18] M. J. Hamp, J. Wright, M. Hubbard, and B. Brimacombe, "Investigation into the temperature dependence of chromatic dispersion in optical fiber," *IEEE Photon. Technol. Lett.*, vol. 14, no. 11, pp. 1524–1526, Nov. 2002, doi: 10.1109/LPT.2002.803902.

[19] D. Sun et al., "Distribution of high-stability 100.04 GHz millimeter wave signal over 60 km optical fiber with fast phase-error-correcting capability," *Opt. Lett.*, vol. 39, no. 10, pp. 2849–2852, 2014, doi: 10.1364/OL.39.002849.